ADVANCED MATERIALS
www.advmat.de

Enhanced Photovoltaic Performance by Modulating Surface Composition in Bulk Heterojunction Polymer Solar Cells Based on PBDTTT-C-T/$PC_{71}BM$

Xia Guo, Maojie Zhang, Wei Ma,* Long Ye, Shaoqing Zhang, Shengjian Liu, Harald Ade, Fei Huang,* and Jianhui Hou**

Recently, the power conversion efficiencies (PCEs) of the bulk heterojunction (BHJ) polymer solar cells, consisting of conjugated polymers as donor and fullerene derivatives as acceptor, have reached up to ~9%.[1] As known, morphology control of active layers of BHJ solar cells plays a critical role affecting the device performance.[2] The ideal morphology formed in the active layer provides not only sufficient interfaces for efficient charge separation but also good percolation pathways for charge carrier transport to the respective electrodes so as to minimize the recombination of free charges.[3] However, the efficient charge collection in a BHJ PSCs can also be assisted by the surface composition of the active layer.[4] For example, the acceptor enrichment in the surface closed to the cathode would block the hole transport to the cathode,[5] and the donor enrichment in the interface closed to the anode would block the electron transport to the anode.[6] Therefore, it is essential to find a method to control not only the bulk morphologies but also the surface composition of the donor-acceptor blend film.

Since the pioneer work reported by Bazan et al.,[7] the addition of solvent additives with high boiling points (*BP*) have attracted much attention and has been used as a simple and effective way to improve the morphology of the active layers of BHJ PSC devices. According to the reported works, the effect of the solvent additives on morphology control is attributed to two properties: their selective solvency to the ingredients in the BHJ layers and their low volatility.[7b,8–11] Therefore, solvent additives like 1, 8-Octanedithiol (OT), 1, 8-Diiodooctane (DIO) and N-methyl pyrrolidone (NMP) have been selectively used to optimize the bulk morphologies of active layers for PSCs based on different polymers.[7–11] However, the effects of additives on the surface compositions of the active layers have not been reported in detail. Considering that the surface composition in BHJ layers plays an important role for charge transport and charge collection in PSCs, we hypothesized that the application of high *BP* solvent additives may be an effective method to control not only the bulk morphology but also the surface composition of the BHJ layers.

In this work, the blend of PBDTTT-C-T (see **Scheme 1**) and [6, 6]-phenyl-C_{71}-butyric acid methyl ester ($PC_{71}BM$) (1:1.5, w/w) was chosen as the model system to explore the effects of variation of surface composition and device structures on photovoltaic performance and also to investigate the mechanism for why the inverted structures[12] are helpful to realize higher PCE in some of PSCs. Since the addition of DIO is a very effective method to improve photovoltaic properties of the PBDTTT-C-T: $PC_{71}BM$ system, herein the blend solvent of *o*-DCB and DIO was used to modulate the bulk morphologies and the surface compositions. In the PSC devices with conventional structure (c-PSC), PEDOT:PSS and Ca were used as the materials for making the buffer layers of the anode and the cathode (HTL and ETL), respectively; in the PSC devices with inverted structure (i-PSC), cross-linked water/alcohol soluble polymer, named as poly[(9,9-bis(3′-(N,N-dimethylamino) propyl)-2,7-fluorene)-alt-2,7-(9,9-bis(3-ethyl-(oxetane-3-ethyloxy)-hexyl)-fluorene)] (PFN-OX),[13] and MoO_3 were used as the ETL and HTL materials, respectively. We found that when DIO was used as the high *BP* additive, the donor material (PBDTTT-C-T) will be relatively enriched on the top surface of the blend film and this surface composition is more favorable to i-PSCs than c-PSCs. As expected, the i-PSC device showed an enhanced PCE of 9.13%, which is much higher than that of the c-PSC device. Overall, this work suggests that when high *BP* solvent additive is used, the BHJ films may have asymmetric surface compositions, and consequently, enhanced photovoltaic performance can be realized by selecting an appropriate device structure.

In our previous work, we found that for the photovoltaic system of PBDTTT-C-T: $PC_{71}BM$, the optimal D/A ratio is 1:1.5 (w/w) and the optimal ratio of DIO/*o*-DCB is 3% (v/v),[14] and the optimal thickness of the blend films is ~100 nm. Since we are focusing on investigating the correlations among the surface compositions, the device structures and the photovoltaic properties, these conditions for fabrication of the blend films

X. Guo, M. Zhang, L. Ye, S. Zhang, J. Hou
State Key Laboratory of Polymer
Physics and Chemistry
Institute of Chemistry
Chinese Academy of Sciences
Beijing 100190, P. R. China
E-mail: zmj2008@iccas.ac.cn; hjhzlz@iccas.ac.cn
W. Ma, H. Ade
Department of Physics
North Carolina State University
Raleigh, North Carolina 27695, USA
E-mail: wma5@ncsu.edu
S. Liu, F. Huang
Institute of Polymer Optoelectronic Materials and Devices
State Key Laboratory of Luminescent Materials and Devices
South China University of Technology
Guangzhou 510640, P. R. China
E-mail: msfhuang@scut.edu.cn
X. Guo, L.Ye
University of Chinese Academy of Sciences
Beijing 100049, P. R. China

DOI: 10.1002/adma.201400411

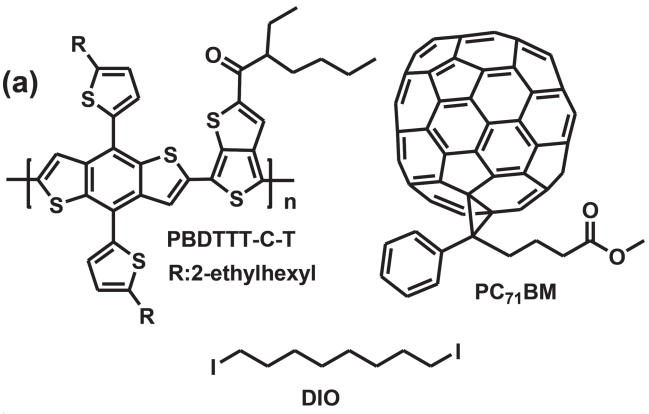

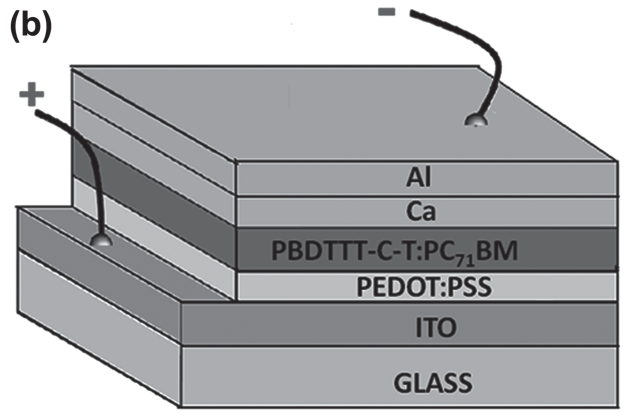

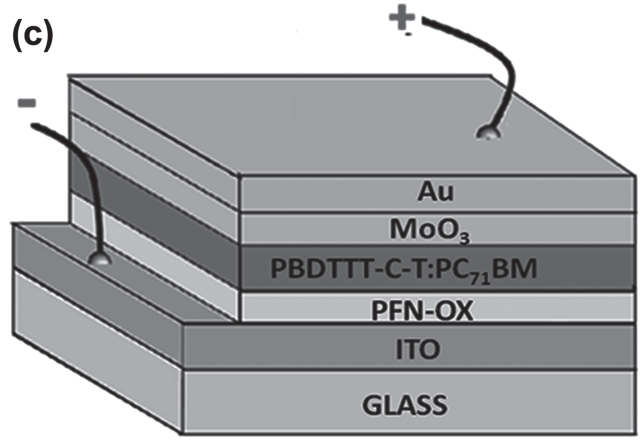

Scheme 1. Molecular structures of PBDTTT-C-T, $PC_{71}BM$ and DIO (a); Schematic of the device structure: the conventional (b) and the inverted (c).

were strictly followed. Initially, atomic force microscopy (AFM) and transmission electron microscopy (TEM) were used to investigate the morphology of the blend films in the real space. As shown in **Figure 1**a and 1d, compared to the blend film processed without DIO, the blend film processed with DIO show higher surface roughness, i.e., the R_q of the blend changed from 0.37 nm to 2.15 nm. Meanwhile, it seems that similar phase separation can be observed Figure 1b and 1e, and no big size aggregation can be distinguished in these two phase images. The TEM images (as shown in Figure 1c and 1f) of these two blends show very low contrast and no distinct phase separation can be observed. Overall, the AFM and TEM results indicate that the PBDTTT-C-T phase has good compatibility with the $PC_{71}BM$ phase, and for the blend films processed without and with DIO, the variations in their morphologies cannot be clearly distinguished by AFM and TEM measurements.

The top surface compositions of the blend films processed without or with using DIO were characterized by X-ray Photoelectron Spectroscopy (XPS).[8c,15] The detailed results of XPS measurements of the blend films are collected in **Table 1** and the spectra are shown in **Figure 2**a. The XPS measurement of the pure polymer film showed an atomic ratio of 8.10 for C 1s and S 2p peaks, which is close to the calculated values of C/S stoichiometric ratio (7.94), indicating that the XPS test can give reliable information of film surface composition. In the PBDTTT-C-T: $PC_{71}BM$ blend, sulfur can be used as the characteristic element of the polymer, because $PC_{71}BM$ does not contain sulfur. Therefore, the higher C/S ratio ($R_{C/S}$) is observed, the more $PC_{71}BM$ is enriched on the top surface. The $R_{C/S}$ value of the blend film processed by pure o-DCB is significantly higher that of the blend film processed by o-DCB/DIO ($R_{C/S,\ o\text{-}DCB} > R_{C/S,\ o\text{-}DCB/DIO}$), meaning that the use of DIO will cause the enrichment of the polymer at the top surface.

Furthermore, surface potentials of the top surfaces of these blend films were investigated by using the Peak Force-Kelvin Probe Force Microscopy (PF-KPFM).[16] The PF-KPFM surface potential images and the corresponding analysis curves of contact potential differences on the top surfaces are shown in Figure 2b. The average surface contact potentials were deduced with a scale of 500 nm. According to the PF-KPFM measurements, the average contact surface potentials (φ) of the blend film casted from pure *o*-DCB was found to be ~0.35 V higher than that of the film with DIO additive. Because the surface energy (γ)[17] of PCBM (~37.8 mN/m^2) higher than that of polymer (~26.9 mN/m^2), we can get that when using DIO as additive, more polymer can be enriched at the surface.

Grazing Incidence Wide-angle X-ray Scattering (GIWAXS) was used to analyze the crystallinity of the PBDTTT-C-T: $PC_{71}BM$ blend films processed without and with the use of DIO. The blend thin films were spin-cast on PSS-treated Si substrates and have a thickness of ~100 nm.[18] **Figure 3**a and 3b show the 2D patterns and the out-of plane and in plane profiles of the films processed with or without additive. The GIWAXS patterns show only broad polymer lamellar reflections (100) at $q \approx 0.3$ Å^{-1} for both two blend films. The $PC_{71}BM$ aggregation peaks are locate at $q \approx 1.3$ Å^{-1}. No clear π–π stacking reflection peak can be observed for the blend films. Both blends films exhibit weak peaks at $q \approx 0.4$ Å^{-1}, which originates from scattering from the PSS when incident angle of x-ray beam is large enough to penetrate the film. As a reference, PSS only film reflection profiles are plotted at the bottom of Figure 3b. In conclusion, these two blend films processed by different solvents show similar and very low crystallinities, implying that the use of DIO has little influence on molecular packing structure in the PBDTTT-C-T: $PC_{71}BM$ blend.

Resonant Soft X-ray Scattering (R-SoXS) is employed to provide detailed statistical information about the bulk morphology of the blend films, i.e., the median characteristic length scales of the morphology and the average composition variations $<\Delta c>$.[19] With the enhanced contrast near carbon

Adv. Mater. **2014**,
DOI: 10.1002/adma.201400411

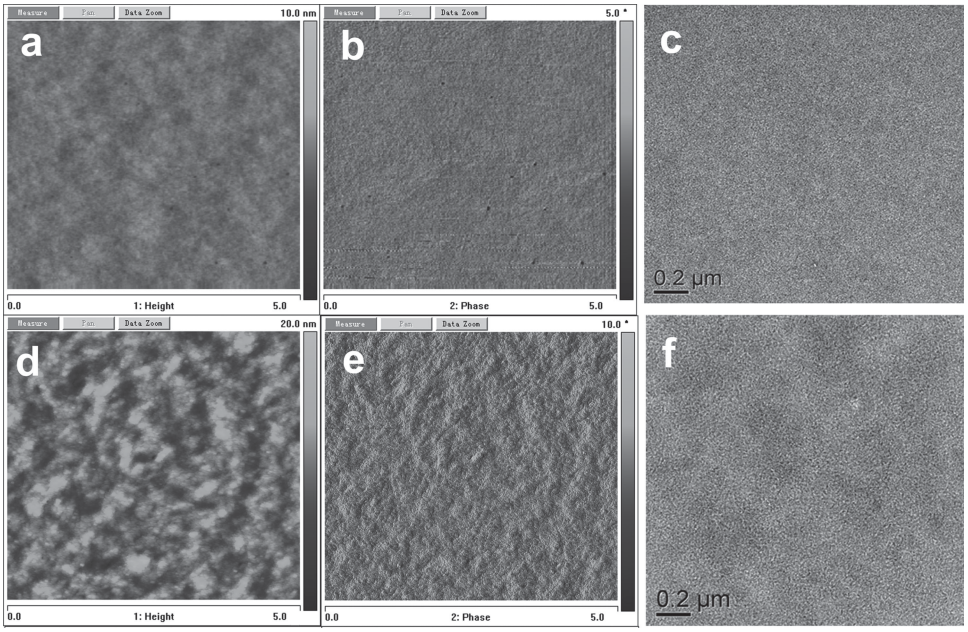

Figure 1. AFM topography images (5 μm × 5 μm) (a, d), AFM phase images (b, e) and TEM images (c, f) of the PBDTTT-C-T: $PC_{71}BM$ blend films (1:1.5, w/w): (a, b, c) for the films processed by pure *o*-DCB; (d, e, f) for the films processed with 3% DIO.

K edge, R-SoXS overcomes the weakness of the AFM and TEM discussed above. A photon energy 284.2 eV was utilized to provide high material contrast between PBDTTT-C-T and $PC_{71}BM$.[19,20] Figure 3c shows the R-SoXS profile of blend films processed with or without additives. The distribution of scattering profile can be fitted by one or two log-normal functions (see Figure S1 in SI) and represents the distribution function of spatial frequency, s ($s = q/2\pi$). The median of the distribution s_{median} corresponds to the characteristic median length scale, ξ, of the corresponding log-normal distributions in real space with $\xi = 1/s_{median}$, a model independent statistical quantity. When the blend film was processed with pure *o*-DCB, the ξ in the blend is 30 nm; when DIO was used as additive, the scattering profile shows two log-normal distributions, and the corresponding ξ are 70 and 30 nm. It is noted that the film processed by *o*-DCB/DIO shows hierarchical structure and exhibits similar phase separation at small length scale comparing with the blends without processed by additive. It is reported the hierarchical structure is a favorable morphology to enhance device performance.[23] The detail characterization of its impact in our system is outside the scope in this work. The average composition fluctuations <Δc> (referred as relative domain purity within a two phase amorphous: amorphous morphology framework as suggested by the WAXS data) can be extracted by integrating the scattering profile and calculating the Total Scattering Intensity (TSI).[20,21c,22] The relative purity is 0.74 and 1 for the blend processed without and with DIO additive, respectively. We find that domains become significant purer when DIO is used as additive. It is noted that the relative purity 1 does not indicate the domains are 100% pure, but is set to equal to ready allow the ratio of the composition variations to be compared. High composition variations are considered beneficial to reduce geminate and non-geminate recombination and consequently aid high FF and J_{sc} in the device.[24]

The c-PSCs with a structure of ITO/PEDOT: PSS (35 nm)/PBDTTT-C-T: $PC_{71}BM$ (1:1.5, w/w) (~100 nm)/Ca (20 nm)/Al (100 nm) and the i-PSCs with a structure of ITO/PFN-OX (~5 nm)/PBDTTT-C-T: $PC_{71}BM$ (1:1.5, w/w) (~100 nm)/MoO_3 (10 nm)/Au (100 nm) as shown in Scheme 1 were fabricated. **Figure 4** shows the current density-voltage (*J*–*V*) curves of the

Table 1. XPS element analysis results of the pure polymer film and the blend films processed without or with the use of DIO.

Film	Processing solvent	C_{1s} (%)	S_{2p} (%)	C/S Ratio	Real D/A ratio on top surface[d)]
Pure polymer	Theoretical value[a)]	87.27	10.99	7.94	1: 0
	Pure *o*-DCB	87.06	10.75	8.10	1: 0
D/A Blend[b)] (w/w = 1:1.5)	Theoretical value[c)]	92.22	4.40	20.96	1: 1.5
	Pure *o*-DCB	91.04	5.74	15.86	1: 0.88
	o-DCB with 3% DIO	89.86	7.33	12.26	1: 0.48

[a)]Theoretical value calculated for $C_{48}H_{56}OS_6$; [b)]the blend films are prepared by the same processes condition as those used in device fabrication; [c)]Theoretical value calculated for **PBDTTT-C-T**/$PC_{71}BM$ (w/w = 1:1.5); [d)]These values are calculated according to the theoretical elemental compositions of C and S or the real C and S compositions obtained from XPS measurements.

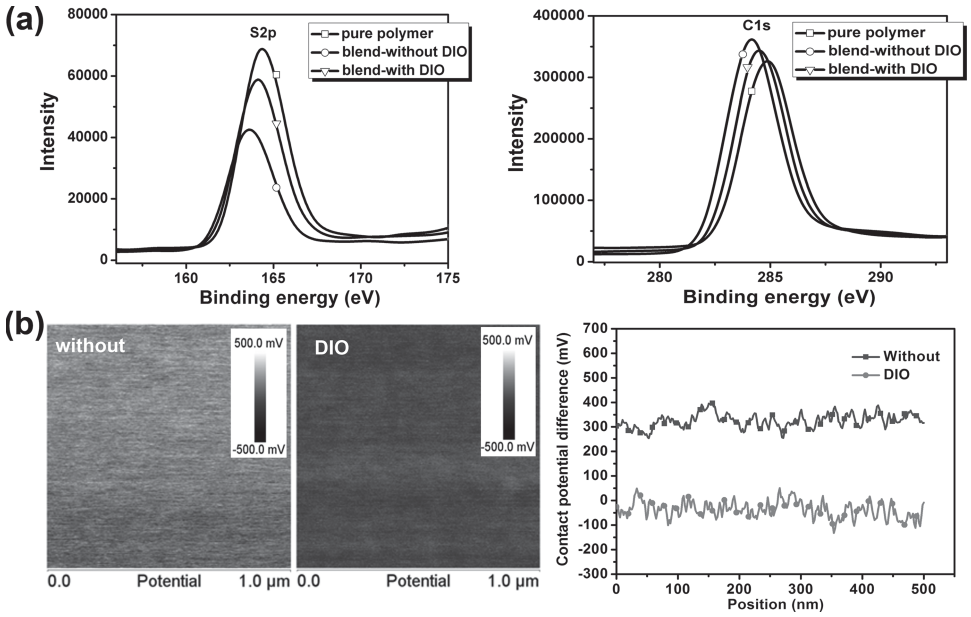

Figure 2. (a) the XPS measurements of the top surfaces of the pure polymer film and the PBDTTT-C-T: $PC_{71}BM$ blend films (1:1.5, w/w) without or with additives; (b) the PF-KPFM surface potential images (1 μm × 1 μm) of PBDTTT-C-T: $PC_{71}BM$ blend films and the analysis curves of the contact potential differences of the top surfaces for the blend films.

PSCs under the illumination of AM 1.5G, 100 mW/cm^2 and the external quantum efficiency (EQE) curves of the devices. The corresponding photovoltaic data of the devices are summarized in **Table 2**.

For c-PSCs, in comparison with the devices processed without DIO, the device processed with DIO shows obvious decrease in V_{OC}, from 0.84 V to 0.76 V, and great increase in J_{SC} and FF, from 13.1 mA/cm^2 to 15.2 mA/cm^2 and 49.8% to 62.3%, respectively. As discussed above, the surface potential of the blend treated by the use of DIO is obvious lower than that of the blend processed without DIO, which should be the main reason for the reduced V_{OC}.[16b,c,25,26] As shown as in Figure S2, Table S1 and Figure 2, compared to the blend processed without DIO, the blend processed with DIO has higher and symmetric hole and electron mobilities and favorable bulk and surface morphologies to keep efficient charge separation and also reduce the non-geminate recombination,[27] and therefore, the J_{SC} and the FF can be simultaneously improved by using DIO as additive.

As known, in a PSC with conventional structure, electrons are transported towards the top surface of the BHJ blend through the channel formed by the acceptor material and then collected by the cathode, so if the donor material is enriched

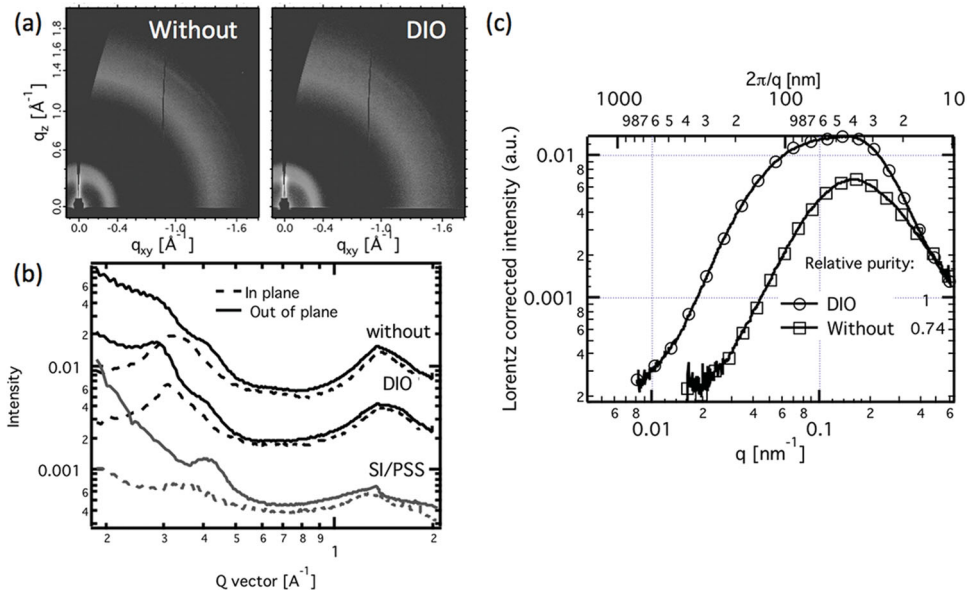

Figure 3. The 2D patterns profiles (a),(b) and the R-SoXS profile (c) of blend films processed with or without additives.

Adv. Mater. **2014**,
DOI: 10.1002/adma.201400411

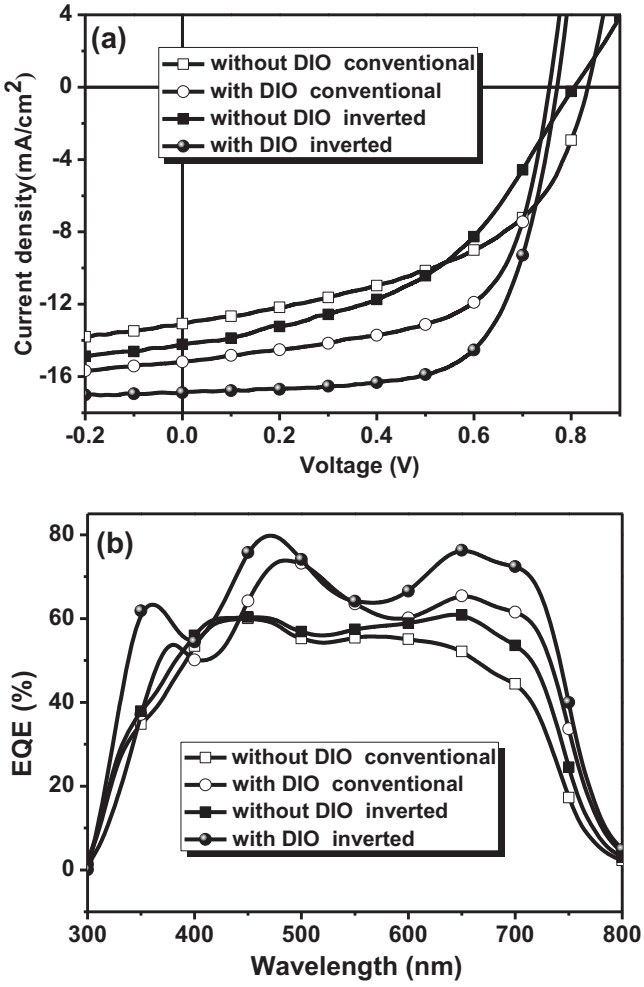

Figure 4. *J–V* curves (a) and EQE (b) of the PSCs based on PBDTTT-C-T: $PC_{71}BM$ (1:1.5, w/w) without or with DIO additive for the conventional device and inverted device, under the illumination of AM 1.5G, 100 mW/cm^2.

near to the interface between the blend and the cathode, i.e., the top surface of the blend in c-PSC, the electron transport and the electron collection will be impeded. Therefore, from the point of view of the top surface composition, the PBDTTT-C-T: $PC_{71}BM$ blend processed with DIO may be more suitable for electron transport and collection in i-PSC than in c-PSC. Therefore, as listed in Table 2, from c-PSC to i-PSC, the FF increased from 62.3% to 67.0%.

Table 2. Photovoltaic performance of the devices based on PBDTTT-C-T: $PC_{71}BM$ (1:1.5, w/w) without or with DIO additive under the illumination of AM1.5G, 100 mW/cm^2.

Device structure	Condition	V_{oc} (V)	J_{sc} (mA/cm^2)	*FF* (%)	*PCE* (*PCE*$_{ave}$[a)]) (%)
c-PSCs	w/o	0.84	13.1	49.8	5.48 (5.39)
	DIO	0.76	15.2	62.3	7.20 (7.10)
i-PSCs	w/o	0.81	14.2	45.1	5.19 (5.10)
	DIO	0.77	17.7	67.0	9.13 (9.00)

[a)]the average PCE is obtained from over 20 devices.

On the other hand, from c-PSC to i-PSC, the buffer layer material for modification of the ITO electrode was changed from PEDOT: PSS to PFN-OX. Since PFN-OX has weaker absorption ranging from 500 nm to 1000 nm as shown in Figure S3 than PEDOT: PSS, the active layers can harvest more sunlight in i-PSC than in c-PSC. As shown in Figure 4b, from 550 nm to 750 nm, quantum efficiencies of the two i-PSCs are higher than these of the two c-PSCs, which agrees well with the reported results.[12a,13b] As shown in Figure S3, it can be seen that the PEDOT: PSS layer shows higher transmittance than the PFN-OX layer in the range from 400 nm to 500 nm, while the former has stronger absorption than the latter in the long wavelength direction beyond 500 nm. Interestingly, although these two buffer layers show different transmittance in different region, for the devices processed by o-DCB/DIO, the EQE values can be improved in the whole response region from c-PSC to i-PSC, indicating that for the active layer processed by o-DCB/DIO, the i-PSC structure is more favorable than the c-PSC structure. In detail, from c-PSC to i-PSC, more improvement in quantum efficiency is observed in long wavelength direction than in short wavelength direction, which should be ascribed to the higher transmittance of the PFN-OX layer at long wavelength region. Overall, both two kinds of blend films processed without and with DIO additive show higher J_{SC} values in i-PSCs than in c-PSCs, i.e., the J_{SC} of the devices processed without and with DIO improved from 13.1 mA/cm^2 to 14.2 mA/cm^2 and from 15.2 mA/cm^2 to 17.7 mA/cm^2, respectively. Overall, when the inverted device structure was used instead of the conventional structure, the PCE of the PSC processed without DIO reduced from 5.48% to 5.19%, while the PCE of the PSC processed with DIO increased from 7.20% to 9.13%.

In summary, we fabricated the conventional structure and inverted structure PSCs based on PBDTTT-C-T/$PC_{71}BM$ as the model system without or with the use of solvent additive DIO. We found that the application of high *BP* solvent additives may be an effective method to control not only the bulk morphology but also the surface compositions in the BHJ layers. After using DIO, the polymer will be enriched near to the top surface of the BHJ layer, which is favorable to the PSCs with inverted structure. The PCE of the inverted PSC with DIO additive reached 9.13% under the illumination of AM1.5G, 100 mW/cm^2, which is much higher that of the device with conventional structure. This work suggests that the bulk morphologies and the surface compositions of the BHJ layers should be considered in designing highly efficient PSCs and also demonstrates a new mechanism for why the PSCs with inverted structures have superiorities in realizing higher photovoltaic performance.

Supporting Information

Supporting Information is available from the Wiley Online Library or from the author.

Acknowledgements

This work was supported by 973 and 863 projects, the National Natural Science Foundation of China (NSFC) and the Science and Technology Commission of Beijing. (Nos. 2014CB643501, 91333204,

2011AA050523, Z131100006013002, 51173189 and 51203168). R-SoXS and GIWAXS measurements and analysis by WM and HA are supported by the US Department of Energy, Office of Science, Basic Energy Science, Division of Materials Science and Engineering under contract DE-FG02–98ER45737. X-ray data is acquired at beamlines 7.3.3 (WAXS)[18] and 11.0.1.2. (R-SoXS)[19] at the Advanced Light Source, which is supported by the Director, Office of Science, Office of Basic Energy Sciences, of the U.S. Department of Energy under Contract No. DE-AC02–05CH11231.

Received: January 25, 2014
Revised: March 1, 2014
Published online:

[1] a) M. J. Zhang, X. Guo, S. Q. Zhang, J. H. Hou, *Adv. Mater.* **2014**, *26*, 1118; b) Z. C. He, C. Zhong, X. Huang, W. Y. Wong, H. Wu, L. Chen, S. Su, Y. Cao, *Adv. Mater.* **2011**, *23*, 4636; c) L. T. Dou, J. B. You, J. Yang, C. C. Chen, Y. J. He, S. Murase, T. Moriarty, K. Emery, G. Li, Y. Yang, *Nat. Photonics* **2012**, *6*, 180; d) M. J. Zhang, Y. Gu, X. Guo, F. Liu, S. Q. Zhang, L. J. Huo, T. P. Russell, J. H. Hou, *Adv. Mater.* **2013**, *25*, 4944; e) J. You, L. Dou, K. Yoshimura, T. Kato, K. Ohya, T. Moriarty, K. Emery, C. C. Chen, J. Gao, G. Li, Y. Yang, *Nat. Commun.* **2013**, *4*, 1446.

[2] a) J. Peet, A. J. Heeger, G. C. Bazan, *Accounts. Chem. Res.* **2009**, *42*, 1700; b) M. J. Zhang, X. Guo, Y. F. Li, *Adv. Energy Mater.* **2011**, *1*, 557; c) M. J. Zhang, X. Guo, W. Ma, S. Q. Zhang, L. J. Huo, H. Ade, J. H. Hou, *Adv. Mater.* **2013**, DOI: 10.1002/adma.201304631; d) W. W. Li, K. H. Hendriks, A. Furlan, W. S. C. Roelofs, S. C. J. Meskers, M. M. Wienk, R. A. J. Janssen, *Adv. Mater.* **2013**, DOI: 10.1002/adma.201304360; e) K. Mullen, T. M. Swager, *Accounts Chem Res* **2008**, *41*, 1085; f) J. W. Chen, Y. Cao, *Acc. Chem. Res.* **2009**, *42*, 1709; g) O. Inganas, F. L. Zhang, M. R. Andersson, *Accounts Chem Res* **2009**, *42*, 1731.

[3] a) B. C. Thompson, J. M. J. Fréchet, *Angew. Chem. Int. Edit.* **2008**, *47*, 58; b) J. A. Bartelt, Z. M. Beiley, E. T. Hoke, W. R. Mateker, J. D. Douglas, B. A. Collins, J. R. Tumbleston, K. R. Graham, A. Amassian, H. Ade, J. M. J. Fréchet, M. F. Toney, M. D. McGehee, *Adv. Energy Mater.* **2013**, *3*, 363.

[4] C. R. McNeill, J. J. M. Halls, R. Wilson, G. L. Whiting, S. Berkebile, M. G. Ramsey, R. H. Friend, N. C. Greenham, *Adv. Funct. Mater.* **2008**, *18*, 2309.

[5] a) G. Li, V. Shrotriya, J. Huang, Y. Yao, T. Moriarty, K. Emery, Y. Yang, *Nat. Mater.* **2005**, *4*, 864; b) J. H. Park, J. S. Kim, J. H. Lee, W. H. Lee, K. Cho, *J. Phys. Chem. C* **2009**, *113*, 17579.

[6] L. Chang, H. W. A. Lademann, J. B. Bonekamp, K. Meerholz, A. J. Moulé, *Adv. Funct. Mater.* **2011**, *21*, 1779.

[7] a) M. M. Wienk, M. Turbiez, J. Gilot, R. A. J. Janssen, *Adv. Mater.* **2008**, *20*, 2556; b) W. W. Li, W. S. C. Roelofs, M. M. Wienk, R. A. J. Janssen, *J. Am. Chem. Soc.* **2012**, *134*, 13787; c) S. Alem, T. Y. Chu, S. C. Tse, S. Wakim, J. P. Lu, R. Movileanu, Y. Tao, F. Belanger, D. Desilets, S. Beaupre, M. Leclerc, S. Rodman, D. Waller, R. Gaudiana, *Org. Electron.* **2011**, *12*, 1788; d) M. J. Zhang, X. Guo, X. C. Wang, H. Q. Wang, Y. F. Li, *Chem. Mater.* **2011**, *23*, 4264; e) F. Liu, Y. Gu, C. Wang, W. Zhao, D. Chen, A. L. Briseno, T. P. Russell, *Adv. Mater.* **2012**, *24*, 3947.

[8] a) J. Peet, J. Y. Kim, N. E. Coates, W. L. Ma, D. Moses, A. J. Heeger, G. C. Bazan, *Nat. Mater.* **2007**, *6*, 497; b) J. K. Lee, W. L. Ma, C. J. Brabec, J. Yuen, J. S. Moon, J. Y. Kim, K. Lee, G. C. Bazan, A. J. Heeger, *J. Am. Chem. Soc.* **2008**, *130*, 3619; c) Y. Yao, J. H. Hou, Z. Xu, G. Li, Y. Yang, *Adv. Funct. Mater.* **2008**, *18*, 1783; d) C. V. Hoven, X. D. Dang, R. C. Coffin, J. Peet, T. Q. Nguyen, G. C. Bazan, *Adv. Mater.* **2010**, *22*, E63; e) K. R. Graham, P. M. Wieruszewski, R. Stalder, M. J. Hartel, J. G. Mei, F. So, J. R. Reynolds, *Adv. Funct. Mater.* **2012**, *22*, 4801.

[9] S. J. Lou, J. M. Szarko, T. Xu, L. P. Yu, T. J. Marks, L. X. Chen, *J. Am. Chem. Soc.* **2011**, *133*, 20661.

[10] a) J. T. Rogers, K. Schmidt, M. F. Toney, E. J. Kramer, G. C. Bazan, *Adv. Mater.* **2011**, *23*, 2284; b) X. Guo, C. Cui, M. Zhang, L. Huo, Y. Huang, J. Hou, Y. Li, *Energy Environ. Sci.* **2012**, *5*, 7943; c) X. Guo, M. J. Zhang, L. J. Huo, C. H. Cui, Y. Wu, Y. Huang, J. H. Hou, Y. F. Li, *Macromolecules* **2012**, *45*, 6930; d) M. S. Su, C. Y. Kuo, M. C. Yuan, U. S. Jeng, C. J. Su, K. H. Wei, *Adv. Mater.* **2011**, *23*, 3315.

[11] a) B. Walker, A. Tamayo, D. T. Duong, X. D. Dang, C. Kim, J. Granstrom, T. Q. Nguyen, *Adv. Energy Mater.* **2011**, *1*, 221; b) X. L. Liu, S. Huettner, Z. X. Rong, M. Sommer, R. H. Friend, *Adv. Mater.* **2012**, *24*, 669; c) K. R. Graham, P. M. Wieruszewski, R. Stalder, M. J. Hartel, J. G. Mei, F. So, J. R. Reynolds, *Adv. Funct. Mate.* **2012**, *22*, 4801; d) A. R. Campbell, J. M. Hodgkiss, S. Westenhoff, I. A. Howard, R. A. Marsh, C. R. McNeill, R. H. Friend, N. C. Greenham, *Nano Lett.* **2008**, *8*, 3942.

[12] a) Z. C. He, C. Zhong, S. Su, M. Xu, H. B. Wu, Y. Cao, *Nature Photonics* **2012**, *6*, 591; b) Z. A. Tan, W. Q. Zhang, Z. G. Zhang, D. P. Qian, Y. Huang, J. H. Hou, Y. F. Li, *Adv. Mater.* **2012**, *24*, 1476; c) S. H. Liao, H. J. Jhuo, Y. S. Cheng, S. A. Chen, *Adv. Mater.* **2013**, *25*, 4766; d) H. Choi, J. S. Park, E. Jeong, G. H. Kim, B. R. Lee, S. O. Kim, M. H. Song, H. Y. Woo, J. Y. Kim, *Adv. Mater.* **2011**, *23*, 2759; e) C. H. Hsieh, Y. J. Cheng, P. J. Li, C. H. Chen, M. Dubosc, R. M. Liang, C. S. Hsu, *J. Am. Chem. Soc.* **2010**, *132*, 4887.

[13] a) S. J. Liu, K. Zhang, J. M. Lu, J. Zhang, H. L. Yip, F. Huang, Y. Cao, *J. Am. Chem. Soc.* **2013**, *135*, 15326; b) Y. Dong, X. W. Hu, C. H. Duan, P. Liu, S. J. Liu, L. Y. Lan, D. C. Chen, L. Ying, S. J. Su, X. Gong, F. Huang, Y. Cao, *Adv. Mater.* **2013**, *25*, 3683; c) C. Zhong, S. Liu, F. Huang, H. Wu, Y. Cao, *Chem. Mater.* **2011**, *23*, 4870.

[14] L. J. Huo, S. Q. Zhang, X. Guo, F. Xu, Y. F. Li, J. H. Hou, *Angew. Chem. Int. Ed.* **2011**, *50*, 9697.

[15] a) Z. Xu, L. M. Chen, G. W. Yang, C. H. Huang, J. H. Hou, Y. Wu, G. Li, C. S. Hsu, Y. Yang, *Adv. Funct. Mater.* **2009**, *19*, 1227; b) R. Kokubu, Y. Yang, *Phys. Chem. Chem. Phys.* **2012**, *14*, 8313.

[16] a) http://www.brukeraxs.com/fileadmin/userupload/webinars/slides/High_Resolution_Quantitative_KPFM_PeakForce_webinar-slides_120822.pdf (accessed June 2013); b) L. Ye, Y. Jing, X. Guo, H. Sun, S. Q. Zhang, M. J. Zhang, L. J. Huo, J. H. Hou, *J. Phys. Chem. C* **2013**, *117*, 14920; c) H. Q. Zhou, Y. Zhang, J. Seifter, S. D. Collins, C. Luo, G. C. Bazan, T.-Q. Nguyen, A. J. Heeger, *Adv. Mater.* **2013**, *25*, 1646.

[17] a) D. S. Germack, C. K. Chan, B. H. Hamadani, L. J. Richter, D. A. Fischer, D. J. Gundlach, D. M. DeLongchamp, *Appl. Phys. Lett.* **2009**, *94*, 233303; b) S. K. Hau, H.-L. Yip, O. Acton, N. S. Baek, H. Ma, A. K.-Y. Jen, *J. Mater. Chem.* **2008**, *18*, 5113; c) H. Li, H. W. Tang, L. G. Li, W. T. Xu, X. L. Zhao, X. N. Yang, *J. Mater. Chem.* **2011**, *21*, 6563.

[18] A. Hexemer, W. Bras, J. Glossinger, E. Schaible, E. Gann, R. Kirian, A. MacDowell, M. Church, B. Rude, H. Padmore, *J. Phys. Conf. Ser.* **2010**, *247*, 012007.

[19] E. Gann, A. T. Young, B. A. Collins, H. Yan, J. Nasiatka, H. A. Padmore, H. Ade, A. Hexemer, C. Wang, *Rev. Sci. Instrum.* **2012**, *83*, 045110.

[20] W. Ma, L. Ye, S. Zhang, J. Hou, H. Ade, *J. Mater. Chem. C* **2013**, *1*, 5023.

[21] a) H. Yan, B. A. Collins, E. Gann, C. Wang, H. Ade, C. R. McNeill, *Acs. Nano.* **2012**, *6*, 677; b) A. C. Stuart, J. R. Tumbleston, H. X. Zhou, W. T. Li, S. B. Liu, H. Ade, W. You, *J. Am. Chem. Soc.* **2013**, *135*, 1806; c) W. Ma, J. R. Tumbleston, M. Wang, E. Gann, F. Huang, H. Ade, *Adv. Energy. Mater.* **2013**, *3*, 864; d) L. Ye, S. Zhang, W. Ma, B. Fan, X. Guo, Y. Huang, H. Ade, J. Hou, *Adv. Mater.* **2012**, *24*, 6335.

[22] B. A. Collins, Z. Li, J. R. Tumbleston, E. Gann, C. R. McNeill, H. Ade, *Adv. Energy Mater.* **2013**, *3*, 65.

[23] W. Chen, T. Xu, F. He, W. Wang, C. Wang, J. Strzalka, Y. Liu, J. Wen, D. J. Miller, J. Chen, K. Hong, L. Yu, S. B. Darling, *Nano Lett.* **2011**, *11*, 3707.
[24] W. Ma, J. Tumbleston, M. Wang, E. Gann, F. Huang, H. Ade, *Adv. Energy Mater.* **2013**, *3*, 864.
[25] X. F. Liu, W. Wen, G. C. Bazan, *Adv. Mater.* **2012**, *24*, 4505.
[26] J. H. Seo, A. Gutacker, Y. M. Sun, H. B. Wu, F. Huang, Y. Cao, U. Scherf, A. J. Heeger, G. C. Bazan, *J. Am. Chem. Soc.* **2011**, *133*, 8416.
[27] a) X. Guo, M. J. Zhang, J. H. Tan, S. Q. Zhang, L. J. Huo, W. P. Hu, Y. F. Li, J. H. Hou, *Adv. Mater.* **2012**, *24*, 6536; b) D. Muhlbacher, M. Scharber, M. Morana, Z. G. Zhu, D. Waller, R. Gaudiana, C. Brabec, *Adv. Mater.* **2006**, *18*, 2884.